

Molecular Structure with Exotic Clusters in light Neutron-rich Nuclei

Y. Kanada-En'yo

*Institute of Particle and Nuclear Studies,
High Energy Accelerator Research Organization,
1-1 Oho, Tsukuba, Ibaraki 305-0801, Japan*

The excited states of ^{12}Be , ^{14}Be and ^{15}B have been studied with a method of antisymmetrized molecular dynamics. In the predicted excited states we find novel molecule-like structures with very exotic clusters such as $^6\text{He}+^8\text{He}$ in ^{14}Be and $^6\text{He}+^9\text{Li}$ in ^{15}B . The origin of the ^6He cluster development in the very neutron-rich nuclei is understood by the new-type correlation among 4 neutrons and 2 protons. In this paper we also present our recent challenge to study *sd*-shell nuclei. Shape coexistence problems in ^{36}Ar and ^{40}Ca are discussed.

§1. Introduction

In the light nuclear region, a clustering aspect is one of the essential features in unstable nuclei as well as in stable nuclei. Owing to the progress of the experimental techniques, information for the excited states of light unstable nuclei have been increased rapidly. The exotic clustering of light unstable nuclei is one of the attractive subjects in the experimental and theoretical researches.

For example, theoretical studies on ^{10}Be ^{1), 2), 3), 4), 5)} suggested molecule-like structures in the excited bands $K = 1_1^-$ and $K = 0_2^+$. The other candidates for the molecule-like states are the excited states of ^{12}Be which have been recently discovered in the break-up reactions into $^6\text{He}+^6\text{He}$ and $^8\text{He}+^4\text{He}$ ⁶⁾. On the other hand, the structure of the ground state of ^{12}Be has been interesting because there are some experimental data which indicate the vanishing of magic number 8 in ^{12}Be ^{7), 8)}. However ^{12}Be has not been studied enough by full microscopic calculations assuming no cluster core. It is also important to search for molecule-like states in other neutron-rich nuclei in order to understand universal features of clustering in unstable nuclei. Our first aim is to study the states covering the ground and the excited ones of light neutron-rich nuclei with antisymmetrized molecular dynamics (AMD). We study the structures of ^{12}Be and challenge to discover possible molecule-like states with exotic clusters in heavier neutron-rich nuclei, ^{14}Be and ^{15}B .

We apply the microscopic method of antisymmetrized molecular dynamics (AMD) which has already proved to be a very useful approach for the structure study of general light nuclei ^{9), 10), 5), 11)}. In the study of ^{12}C ¹⁰⁾, the author has proposed a new version of the method, variation after spin-parity projection (VAP) in the AMD framework which is very useful to investigate excited states with various kinds of structures such as spherical shell-model-like structures and clustering structures. The author and her collaborators have succeeded to describe the structures of excited states of ^{10}Be ¹⁾ with the VAP calculations in the framework of AMD. AMD is the

method that is very suitable to search for the possible exotic clusters in foreign nuclei because we do not need any model assumptions such as the existence of clusters.

As mentioned above, clustering is an important feature in very light nuclei. However it is an open problem whether or not clustering effects are seen also in unstable *sd*-shell nuclei. I challenge to study structures of *sd* nuclei with AMD method. In this paper, the recent hot subjects of shape coexistence problems in ^{36}Ar and ^{40}Ca have been studied with AMD. Although they are stable ones, the studies of stable nuclei are very essential to investigate the unstable *sd*-shell nuclei.

In this paper, the structures of the excited states of light neutron-rich nuclei, ^{12}Be , ^{14}Be and ^{15}B are studied in Sec.3. We discuss the mechanism of the clustering development from the view point of correlation among nucleons in the single particle orbits. In the study of heavier nuclei with AMD, the shape coexistence problems in ^{36}Ar and ^{40}Ca are investigated in Sec.4.

§2. Formulation

An AMD wave function is a Slater determinant of Gaussian wave packets;

$$\Phi_{AMD} = \frac{1}{\sqrt{A!}} \mathcal{A}\{\varphi_1, \varphi_2, \dots, \varphi_A\}, \quad (1)$$

$$\varphi_i = \phi_{\mathbf{Z}_i} \chi_i \tau_i : \begin{cases} \phi_{\mathbf{Z}_i}(\mathbf{r}_j) \propto \exp \left[-\nu \left(\mathbf{r}_j - \frac{\mathbf{Z}_i}{\sqrt{\nu}} \right)^2 \right], \\ \chi_i = \begin{pmatrix} \frac{1}{2} + \xi_i \\ \frac{1}{2} - \xi_i \end{pmatrix}. \end{cases} \quad (2)$$

where the centers of Gaussians \mathbf{Z}_i 's are complex variational parameters. χ_i is an intrinsic spin function represented by ξ_i which is also a variational parameter specifying the direction of the *i*-th intrinsic spin. τ_i is an isospin function which is fixed to be up(proton) or down(neutron) in the present calculations.

In order to obtain wave function of an excited states of light nucleus, we vary the parameters \mathbf{Z}_i and ξ_i ($i = 1 \sim A$) to minimize the energy expectation value for the parity and total angular momentum eigenstate (VAP calculations),

$$\frac{\langle P_{MK'}^J \Phi_{AMD}^\pm | H | P_{MK'}^J \Phi_{AMD}^\pm \rangle}{\langle P_{MK'}^J \Phi_{AMD}^\pm | P_{MK'}^J \Phi_{AMD}^\pm \rangle}, \quad (3)$$

where the operator of total angular momentum projection $P_{MK'}^J$ is $\int d\Omega D_{MK'}^{J*}(\Omega) R(\Omega)$. The integration for Euler angle Ω is calculated numerically. We adopt the frictional cooling method⁹⁾ to obtain the minimum energy states. Thus we can obtain the lowest state for a given spin parity J^\pm with VAP calculations. For higher excited states we perform the energy variation for the orthogonal component to the lower states by superposing wave functions. More details of the AMD method for the excited states with the variation after spin-parity projection are described in Refs^{10), 5)}. By making VAP calculations for the lowest and the higher excited states with various sets of

total spin and parity $\{J^\pm\}$, we obtain a lot of AMD wave functions $\{\Phi_1, \dots, \Phi_m\}$, which approximately describe the intrinsic states of the corresponding J_n^\pm states. The number m is the number of the considered states. Final results are attained by diagonalizing a Hamiltonian matrix $\langle P_{MK'}^{J^\pm} \Phi_i | H | P_{MK''}^{J^\pm} \Phi_j \rangle$ ($i, j = 1 \sim m$).

For the structure study of heavier nuclei such as ^{36}Ar and ^{40}Ca , we make variation after parity projection but no spin projection (VBP) with a constraint AMD instead of full VAP calculations to save computational time. The adopted constraint in the present calculations is that the expectation values of total oscillator quanta must equal to a given number as $\langle aa^\dagger \rangle = W$. After VBP calculations with a constraint, we make spin projection to obtain a energy curve as a function of total oscillator quanta. The obtained states are superposed by diagonalizing Hamiltonian Matrix $\langle P_{MK'}^{J^\pm} \Phi_i | H | P_{MK''}^{J^\pm} \Phi_j \rangle$.

§3. Results of ^{12}Be , ^{14}Be and ^{15}B

We apply the AMD method for the excited states of ^{12}Be , ^{14}Be and ^{15}B . The adopted interactions in this work are the central force of the modified Volkov No.1 with case 3¹²⁾, the spin-orbit force of G3RS¹³⁾ and the Coulomb force. The Majorana parameter used here is $m = 0.65$, and the strength of G3RS force is chosen to be $u_1 = -u_2 = 3700$ MeV. We choose a optimum width parameter ν for the Gaussians of the single particle wave functions of each nucleus. With these parameters, the parity inversion of the ^{11}Be ground state can be reproduced. The binding energies of ^{12}Be , ^{14}Be and ^{15}B are 61.9 MeV, 59.7 MeV and 73.1 MeV, which are smaller than the experimental data 68.65 MeV, 69.77 MeV, 88.19 MeV, respectively. We have checked that the underestimation with the present interaction parameters can be improved easily by using smaller Majorana parameter as $m = 0.61$. With this parameter set the binding energy of ^{14}Be is 67.7 MeV which well agrees to the experimental data. We also find that the excitation energy of 0_2^+ in ^{14}Be calculated with $m = 0.61$ is 4.2 MeV which is almost as same as the one with $m = 0.65$.

In the calculated results of ^{12}Be with AMD, a lot of excited states appear in the low-energy region. The energy levels of ^{12}Be are presented in Fig. 1. The theoretical levels of 4_2^+ , 6_2^+ and 8_1^+ states well correspond to the recently observed excited states⁶⁾. By analyzing the intrinsic AMD wave functions, we can classify the excited states into rotational bands such as $K^\pi = 0_1^+, 0_2^+, 0_3^+, 1_1^-$. The interesting point is that the newly observed levels⁶⁾ at the energy region above 10 MeV have been found to belong to the third rotational band $K^\pm = 0_3^\pm$. It is also interesting to see the ground $K^\pm = 0_1^\pm$ band properties because the vanishing of the neutron magic number $N = 8$ occurs in ^{12}Be . Even though the ^{12}Be is a neutron magic nucleus with $N = 8$, the intrinsic state of the ground 0^+ state is not the ordinary state with the closed neutron p -shell, but a prolately deformed state with a developed clustering structure, which is dominated by $2p - 2h$ configurations in terms of single-particle orbits. As a result, the ground $K^\pi = 0^+$ band starts from the ground 0^+ state and reaches the band terminal at $J^\pi = 8^+$ with the highest spin state in the $2\hbar\omega$ configurations. On the other hand, the neutron p -shell closed states with $0\hbar\omega$ configurations construct the second $K^\pi = 0_2^+$ band which consists of the second

0^+ and the second 2^+ states. For an experimental evidence, the strength of the β decay from $^{12}\text{Be}(0_1^+)$ to $^{12}\text{B}(1^+)$ is helpful to estimate the breaking of the neutron p -shell⁷⁾. As is expected, the theoretical value of $B(\text{GT})=0.8$ is enough small as the experimental data $B(\text{GT})=0.59$ because the component of the p -shell broken state in the parent $^{12}\text{Be}(0_1^+)$ makes the expectation value of Gamow-Teller operator to be small. It is consistent with the pioneer works^{14), 7)}. It should be pointed out that this is the first theoretical work which can reproduce systematically the energy levels from the ground state to the highly excited states. We have predicted the new $K^\pi = 0_3^+$ rotational band from 0_3^+ , 2_3^+ , 4_2^+ , 6_2^+ and 8_1^+ states. The 0_3^+ state has the mostly developed ${}^6\text{He}+{}^6\text{He}$ clustering. The developed clustering becomes weak gradually with the increase of the total-angular momenta J , and finally it changes to the same spin aligned state at $J^\pm = 8_1^+$ as the one in the $K = 0_1^+$ band. The reason for the spin alignment at $J^\pm = 8^+$ is because the states in the $K^\pm = 0_3^+$ band are the other $2\hbar\omega$ states which must have the same highest spin state as the one in the ground band at the band terminal 8^+ . Although the other evidence for the magic number vanishing is the low-lying 1^- state which has been measured recently⁸⁾, the excitation energy of 1^- state is overestimated in present calculation. The mechanism of energy gain of negative parity states has been still an open problem.

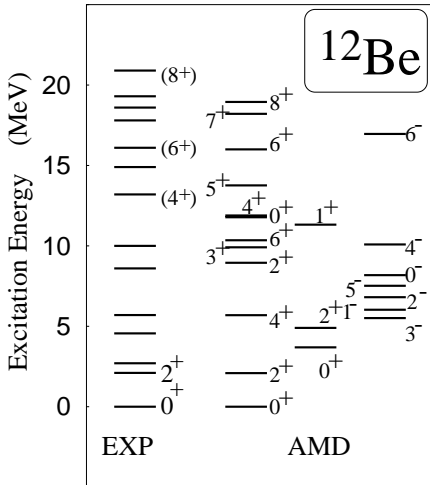


Fig. 1. Excitation energies of the levels in ^{12}Be . Theoretical results are calculated by VAP calculations based on AMD. Experimental data are taken from the Table of Isotopes and Refs 15), 6).

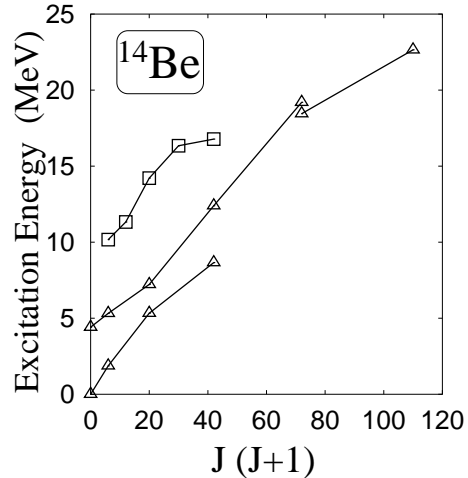


Fig. 2. Excitation energies of the levels in ^{14}Be calculated by VAP calculations based on AMD. Excitation energies are plotted as a function of $J(J+1)$ where J is a total spin of the state.

By analyzing the single particle wave functions in the intrinsic state, the mechanism of the clustering development in the first 0^+ state can be understood by an idea of molecular orbits surrounding 2α cores. Although the molecular orbits in ^{12}Be have been suggested theoretically^{16), 4)}, the important point of the present work is that the structure of 2α cores and surrounding neutrons in ^{12}Be is formed auto-

matically in the energy variation though the existence of any clusters nor molecular orbits is not assumed. On the other hand, it is natural to consider the third 0^+ state as ${}^6\text{He}+{}^6\text{He}$ clustering structure instead of the α and surrounding neutrons because the distance between two clusters is too far to be described in terms of the molecular orbits. In this case, an α cluster goes outward far enough to form a ${}^6\text{He}$ cluster in the correlation with 2 valence neutrons.

Next we present the results of ${}^{14}\text{Be}$. Figure 2 shows the energy levels of the positive parity states of ${}^{14}\text{Be}$. While few excited states are known experimentally, many excited states are predicted in the theoretical results. There are very recent experimental data¹⁷⁾ of a few levels just above the threshold energy (9.1 MeV excitation) for the separation into ${}^8\text{He}$ and ${}^6\text{He}$.

The excited states in the region $J \leq 6$ are classified into 3 rotational bands, $K = 0_1^+$, $K = 0_2^+$ and $K = 2^+$. In most of the states in ${}^{14}\text{Be}$, 2α cores are formed in the calculated results. As a result, 0_1^+ and 0_2^+ states have prolate deformations with the deformation parameters $\beta = 0.49$ and $\beta = 0.64$ respectively. By analyzing the single particle wave functions of the intrinsic states, we found that all the states in the $K = 0_1^+$ and $K = 2^+$ bands are dominated by the normal $0\hbar\omega$ configurations. What is interesting is the exotic clustering structure of the excited states in the second $K^\pi = 0_2^+$ band which comes from $2\hbar\omega$ configurations. In the present calculations, this band is predicted to start from the second $J^\pm = 0_2^+$ state at about 5 MeV and to reach the 8_2^+ state. They have the well-developed ${}^8\text{He}$ and ${}^6\text{He}$ clusters which are very neutron-rich nuclei themselves. The surface cut for the matter density $\rho \geq 0.16$ nucleons/fm³ of the intrinsic state of 0_2^+ state is shown in Fig. 3(a). The ${}^8\text{He}({}^6\text{He})$ cluster is clearly seen in the right(left)-handed side in Fig. 3(a) where the surrounding low density region is omitted. As seen in the figure, the spatial clustering develops remarkably. It is interesting that we can find an origin of the clustering in the single particle wave functions. According to the analysis of the energies and behaviors of the single particle wave functions, the highest 4 neutron orbits correspond to *sd*-like orbits in the deformed system. Roughly speaking, a pair of spin up and down neutrons occupies a higher spatial *sd*-like orbit and the other pair of neutrons occupies the lower spatial orbit. Fig. 3(b) and Fig. 3(c) shows the two types of the spatial orbits for the 4 valence neutrons which contain more than 80 % components of positive parity states. It is found that the 4 neutrons occupy the *sd*-like orbits modified in the prolately deformed system. If we call the longitudinal direction of the prolate deformation as *z*-axis, the highest nucleon orbit seen in Fig. 3(b) is associated with the *sd* orbit with a form of $yz \exp[-\nu r^2]$ which has nodes for the rotation at the *x*-axis. On the other hands, the spatial orbit for the lower one is similar to the orbit of $z^2 \exp[-\nu r^2]$ which has nodes along a *z*-axis (Fig. 3(c)). These neutron orbits are stabilized due to the development clustering structures because they gain their kinetic energies of the nodes along the *z*-axis. From such a viewpoint of the single neutron orbits we can consider that four neutrons in *sd*-like orbits and 2 protons in *p*-like orbits forms a ${}^6\text{He}$ cluster out of a ${}^8\text{He}$ core. In another word, the extremely developed ${}^6\text{He}$ cluster is originated from a new-type correlation among 4 neutrons in *sd* shell and 2 protons in *p* shell.

In the theoretical results of ${}^{15}\text{B}$, we find an exotic clustering ${}^9\text{Li}+{}^6\text{He}$ structure

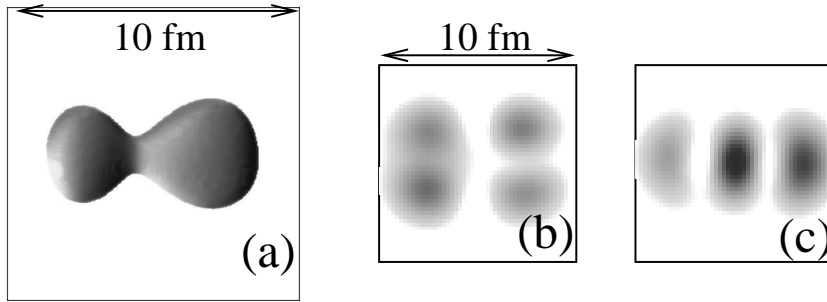


Fig. 3. Intrinsic structure of 0_2^+ of ^{14}Be . Figure (a) shows a surface cut of the matter density $\rho \geq 0.16$ nucleons/ fm^3 . The density is calculated for the intrinsic AMD wave function before spin-parity projection. Density distributions for the single particle orbits of the valence neutrons are presented in the figures (b) and (c).

in the states in the second $K^\pi = 3/2_2^-$ band which starts from the $J^\pm = 3/2_2^-$ state about 5 MeV higher than the ground state. The clusters of $K^\pi = 3/2_2^-$ band are also exotic nuclei ^9Li and ^6He , and develop as remarkably as those in the $K^\pi = 0_2^+$ band of ^{14}Be . The mechanism of the ^6He clustering development in ^{15}B can be also described as the correlation among 4 neutrons in the sd -shell with 2 protons in the p -shell as similar way as ^{14}Be . That is to say that these excited states with $^9\text{Li}+^6\text{He}$ clustering are based on the $4p - 2h$ state of the neutron p -shell. The spatial orbits of 4 valence neutrons are very similar as those of ^{14}Be presented in Figs 3(b) and 3(c). The correlation among 4 neutrons with 2 protons is very unique even though the correlation among two neutrons and two protons has been sometimes discussed in relation with an α cluster. In this paper, we suggest one of the novel feature that 4 neutrons in the sd -shell with 2 protons in the p -shell correlate to form a developed ^6He cluster in the neutron rich nuclei. It is an exciting problem whether or not the ^6He cluster formation may appear in other neutron-rich nuclei.

Since the present results are obtained within the bound state approximation, particle decay width has not been discussed though they are important for the stability of the excited states. Newly predicted states in $K = 0_2^+$ of ^{14}Be are expected to decay into the $^8\text{He}+^6\text{He}$ channel because of the developed clustering. We have calculated the partial decay width of ^{14}Be only for the $^8\text{He}+^6\text{He}$ channel with a method of reduced width amplitude, and found that the widths of 6_2^+ and 8_2^+ states are less than 50 keV. For more detailed analysis of the total width including neutron decays and excited He decays, we require other microscopic frameworks such as a complex scaling method.

§4. Shape coexistence of ^{36}Ar , ^{40}Ca

In the previous section, structures of light neutron-rich have been discussed. Also in neutron-rich sd -shell nuclei we know many interesting phenomena such as vanishing of neutron magic number $N = 20$ in ^{32}Mg . For study of the structures of neutron-rich nuclei, it is very useful to make systematic study associating unstable

nuclei with stable nuclei. For example, let us consider a problem of p -shell nuclei, the magic number $N = 8$ disappearance in ^{12}Be . The intruder ground state is considered to have 2 particles and 2 holes in neutron p -shell. We have already known the similar neutron configuration in the 0_2^+ state of ^{16}O which is described in terms of $4p - 4h$ state with $^{12}\text{C} + \alpha$ clustering. It is very interesting to imagine the structure change when the system varies from $^{16}\text{O}(0_2^+)$ to ^{12}Be with decrease of proton number of the system. In case of sd -shell nuclei, we think that it is helpful to compare the structures of stable nuclei near ^{40}Ca with those of ^{32}Mg to solve the mechanism of neutron magic number vanishing in neutron-rich sd -shell nuclei. Fortunately many rotational bands of ^{36}Ar and ^{40}Ca have been discovered with the recent γ -ray measurements. In this section, the study of the excited states of sd -shell nuclei ^{36}Ar and ^{40}Ca is presented. We discuss the shape coexistence problem of these nuclei which is one of the recent hot subjects.

For the structure study of sd -shell nuclei such as ^{36}Ar and ^{40}Ca , we make variation after parity projection but no spin projection (VBP) with AMD under a constraint on the total oscillator quanta as mentioned in Sec.2. The interactions with a finite-range 3-body force are adopted because the ordinary effective forces such as the MV1 force and the Gogny force are not appropriate to describe the binding energies and radii of nuclei covering wide mass number region from α to ^{40}Ca simultaneously. The central part of present interactions are as follows,

$$V_{\text{central}} = \sum_{i < j} V^{(2)} + \sum_{i < j < k} V^{(3)}, \quad (4)$$

$$V^{(2)} = (1 - m + bP_\sigma - hP_\tau - mP_\sigma P_\tau) \left\{ V_a \exp\left[-\left(\frac{r_{12}}{r_a}\right)^2\right] V_b \exp\left[-\left(\frac{r_{12}}{r_b}\right)^2\right] \right\} \quad (5)$$

$$+ V_c \exp\left[-\left(\frac{r_{12}}{r_c}\right)^2\right], \quad (6)$$

$$V^{(3)} = V_d \exp[-d(r_{12}^2 + r_{23}^2 + r_{31}^2)^2], \quad (7)$$

$$V_a = -198.34 \text{ MeV}, V_b = 300.86 \text{ MeV}, V_c = 22.5 \text{ MeV}, \quad (8)$$

$$r_a = 1.2 \text{ fm}, r_b = 0.7 \text{ fm}, r_c = 0.9 \text{ fm}, V_d = 600 \text{ MeV}, d = 0.8 \text{ fm}^{-2} \quad (9)$$

$$m = 0.193, b = -0.185, h = 0.37, \quad (10)$$

where the ranges and strength parameters are chosen so as to reproduce reasonably the sizes of α and ^{40}Ca , and the binding energies of α , ^{16}O and ^{40}Ca . To choose interaction parameters the other important features like $\alpha + \alpha$ phase shift and saturation property of the symmetric nuclear matter have been taken into consideration. In the total interaction, the spin orbit force of G3RS with the strength $u_{ls} = 2500$ MeV and coulomb force are added to the central force.

First the excited states of ^{36}Ar are studied by VBP calculations with a constraint on the total oscillator quanta \mathcal{N} . Here $\Delta\mathcal{N}$ is defined by the deviation from the minimum oscillator quanta of the system; $\Delta\mathcal{N} = \mathcal{N} - \mathcal{N}_{\text{min}}$, where \mathcal{N}_{min} is 52 in case of ^{36}Ar . After spin projection, we obtain an energy surface as a function of $\Delta\mathcal{N}$. It is found that there is a minimum point in the energies of 0^+ states at $\Delta\mathcal{N} = 1$, which corresponds to the ground state with a normal configuration. By diagonalizing with

the ground state, we obtain the excited state with $4\hbar\omega$ configurations at $\Delta\mathcal{N} = 4$ as a local minimum state. As a result, some rotational bands are constructed. In the ground $K = 0^+$ band the intrinsic state has a normal oblate deformation. On the other hand the largely deformed state with $4\hbar\omega$ configurations makes excited rotational bands $K = 0^+$ and $K = 2^+$. In spite of the highly excited configurations the excited $K = 0^+$ band starts from low energy region about 5 MeV and reaches high spin states $J \geq 16$. This excited $K = 0^+$ band corresponds well to the experimental data observed recently with γ -ray transitions measurements¹⁸⁾. The intrinsic state of the excited band deforms prolately as $\beta = 0.3$. It is interesting that another shape may coexist at $\Delta\mathcal{N} = 5$. Namely, the triaxial shape with pentagon component appears to make another $J^\pm = 10^+$ state at about 10 MeV in present calculations.

In case of ^{40}Ca , the calculations suggest that various kinds of shapes coexist in low energy region although ^{40}Ca is a doubly magic nucleus. First we find the ground state with $0\hbar\omega$ configuration at $\Delta\mathcal{N} = 2$. It has spherical shape (a) as is expected. With the increase of oscillator quanta $\Delta\mathcal{N}$, we obtain energetically stable states with $4\hbar\omega$ configurations at $\Delta\mathcal{N} = 5$. One has an oblate shape (b) and the other has a prolate shape (c). Both intrinsic states construct rotational bands as shown in Fig.4. In the figure only the excitation energies of the states with $J \leq 16$ are presented because of the limitation of computational calculations of spin projection. As the value $\Delta\mathcal{N}$ increases, finally a super deformation (d) appears at $\Delta\mathcal{N} = 10$. By analyzing the single particle wave functions the super deformed state is found to be dominated by $8\hbar\omega$ configurations. The deformation parameter is $\beta \sim 0.4$. It is surprising that the rotational band $K = 0^+$ given from the super deformation starts from the low energy region about 8 MeV excited in spite of the highly excited configurations of the doubly magic nucleus. As a result, many shapes coexist in ^{40}Ca . It is suggested that the spherical ground state, the oblate excited state, the normal prolate excited state, and the prolate super deformed state appear in low energy region. Actually there exist many rotational bands in the experimental data measured recently¹⁹⁾. The calculated super deformed band is considered to be the recently discovered rotational band from 5.273 MeV in the experimental data. Although the level spacing of the super deformed band is overestimated by present calculations, the results should be improved by extended calculations such as cranking methods and GCM calculations along the constraint $\Delta\mathcal{N}$.

In the intrinsic states of the excited states, very strange shapes are found. Figure 5 shows the density distributions of the intrinsic states of the excited bands. A hexagon like three leaves clover shape appears in the oblate state (b), while the super deformed state (d) has a parity asymmetric shape like a pear. One of the origins of such exotic shapes is clustering effects due to ^{12}C clusters.

As mentioned above, many exotic shapes in the positive parity states are suggested in the present calculations. The appearance of a pear-like shape is an exciting prediction because the existence of parity asymmetric shapes in such heavy nuclei as ^{40}Ca is an open problem. In order to confirm the parity asymmetric shapes it is very important to find parity doublet states in negative parity states. As is expected we find the parity doublet states of the super deformation with a pear shape. Also in the negative parity states, many shapes are found in the theoretical results. We

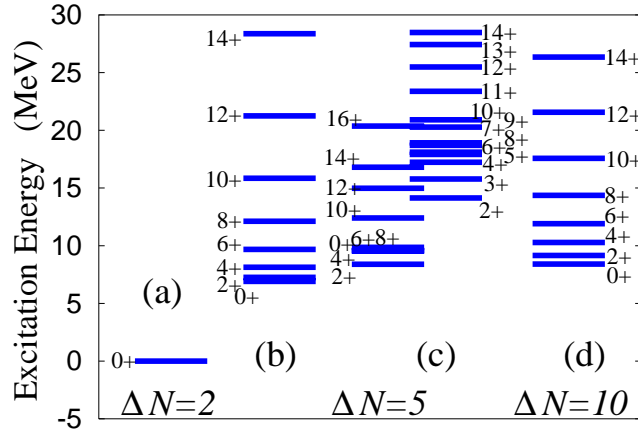


Fig. 4. Theoretical results of energy levels of positive parity states of ^{40}Ca .

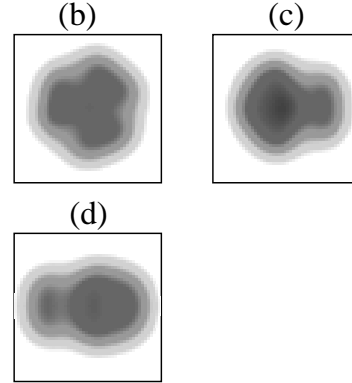


Fig. 5. Density distributions of the intrinsic states of the rotational bands. Figures (b), (c) and (d) correspond to the oblate shape, the prolate shape and the super deformation, respectively.

consider the obtained $K = 0^-$ at $\Delta\mathcal{N} \approx 8$ is the parity doublet of the super deformed band (d) because the intrinsic state is similar to each other. The excitation energy of the band head 1^- state is 12 MeV which is about 3 MeV higher than the energy of 0^+ state in the super deformation band. Present results indicate the possibility of the parity asymmetry shape due to clustering effects in heavier system.

§5. Summary

In summary, we have studied the structure of the excited states of ^{12}Be , ^{14}Be and ^{15}B with variation after spin-parity projection based on the framework of AMD method. We have also reported our recent study of shape coexistence problems in ^{36}Ar and ^{40}Ca with a constraint AMD. We have obtained a variety of exotic structures concerning with clustering.

Various clustering structures in the excited states have been found in the theoretical results in which we have succeeded to reproduce well the excitation energies of many levels of ^{12}Be . The breaking of the neutron magic number $N = 8$ in ^{12}Be has been found. The recently measured excited states are described by the third $K^\pi = 0_3^+$ band which has a foreign clustering structure with developed ^6He and ^6He clusters. Exotic clustering structures such as $^8\text{He}+^6\text{He}$ and $^9\text{Li}+^6\text{He}$ have been predicted in ^{14}Be and ^{15}B , respectively. The formation of the remarkable ^6He clusters can be understood by an unique idea of the new type correlation among 4 neutrons in sd -shell and 2 protons in p -shell. This is the first full microscopic calculation which shows the exotic clustering in the excited states of ^{12}Be , ^{14}Be and ^{15}B . The results suggest an important feature that the exotic clustering structures may exist very often in the excited states of neutron-rich nuclei.

Structures of ^{36}Ar and ^{40}Ca have been studied. In the results it is suggest that

many kinds of shapes coexist in these nuclei. In ^{40}Ca , the spherical ground state, the normal prolate state, the oblate shape, and the prolately super deformation have been found. The prolate state and oblate state are dominated by $4\hbar\omega$ configurations, while the super deformation originates from $8\hbar\omega$ configurations. It is surprising that the rotational bands made of such highly excited configurations start at low excitation energies. The rotational band of the super deformation corresponds to the experimentally measured band which were observed recently in γ ray transitions. In the theoretically obtained intrinsic states, very strange shapes are predicted in the excited states. It is very interesting that parity asymmetric shape like a pear is proposed in the super deformation. Although the negative parity bands have not been confirmed experimentally yet, present results predict that the parity doublet band with negative parity may exist at about 3 MeV higher than the positive parity band.

If we vary the system from ^{40}Ca to ^{32}Mg by decreasing the proton number, how do the structures of the excited states of stable nuclei change? Does the excited state with $4p - 4h$ in the neutron shell appear in ^{32}Mg ? It is a very interesting subject to study structures of intruder states in neutron-rich nuclei associating with the excited of stable nuclei.

Acknowledgements

I would like to thank Prof. H. Horiuchi for many discussions. I am also thankful to Dr. N. Itagaki, Prof. W. Von Oertzen and Prof. Y. Akaishi for helpful discussions and comments. Valuable comments of Prof. S. Shimoura and A. Saito are also acknowledged. The computational calculations of this work are supported by RCNP in Osaka University, YITP in Kyoto University and IPNS/KEK.

References

- [1] Y. Kanada-En'yo, H. Horiuchi and A. Doté, J. Phys. G, Nucl. Part. Phys. **24** 1499 (1998).
- [2] Y. Ogawa, K. Arai, Y. Suzuki, and K. Varga, Nucl. Phys. **A673** 122 (2000).
- [3] A. Doté, H. Horiuchi, and Y. Kanada-En'yo, Phys. Rev. C **56**, 1844 (1997).
- [4] N. Itagaki and S. Okabe, Phys. Rev. C **61**, 044306 (2000).
- [5] Y. Kanada-En'yo, H. Horiuchi and A. Doté Phys. Rev. C **60**, 064304(1999)
- [6] M. Freer, et al., Phys. Rev. Lett. **82**, 1383 (1999).
- [7] T. Suzuki and T. Otsuka, Phys. Rev. bf C 56, 847(1997).
- [8] H. Iwasaki, et al., Phys.Lett.**B 491**, 8(2000).
- [9] Y. Kanada-En'yo, H. Horiuchi and A. Ono, Phys. Rev. C **52**, 628 (1995); Y. Kanada-En'yo and H. Horiuchi, Phys. Rev. C **52**, 647 (1995).
- [10] Y. Kanada-En'yo, Phys. Rev. Lett. **81**, 5291 (1998).
- [11] Y. Kanada-En'yo and H. Horiuchi, to be published in Prog. Theor. Phys. Suppl..
- [12] T. Ando, K.Ikeda, and A. Tohsaki, Prog. Theor. Phys. **64**, 1608 (1980).
- [13] N. Yamaguchi, T. Kasahara, S. Nagata, and Y. Akaishi, Prog. Theor. Phys. **62**, 1018 (1979); R. Tamagaki, Prog. Theor. Phys. **39**, 91 (1968).
- [14] N. Itagaki, S. Okabe and K. Ikeda, Phys. Rev. C **62**, 034301 (2000).
- [15] A.A. Korshennikov, et al., Phys. Lett. B343, 53 (1995).
- [16] W. von Oertzen, Z. Phys. A **354**, 37 (1996).
- [17] A. Saito and S. Shimoura, private cominucations.
- [18] C.E.Svensson et al., Phys.Rev.C**63**, 061301 (2001)
- [19] E.Ideguchi et al.,PHys.Rev.Lett.**87**, 222501(2001)